Available online at www.sciencedirect.com
ScienceDirect
Journal of Asian Earth Sciences 29 (2007) 253–265
Journal of Asian Earth Sciences
www.elsevier.com/locate/jaes

Displacement and timing of left-lateral faulting in the Kunlun Fault Zone, northern Tibet, inferred from geologic and geomorphic features

Bihong Fu [a,*], Yasuo Awata [b]

[a] State Key Laboratory of Lithospheric Evolution, Institute of Geology and Geophysics, Chinese Academy of Sciences, P.O. Box 9825, Beijing 100029, PR China
[b] Active FaultResearch Center, AIST, Tsukuba 305-8567, Japan

Received 28 December 2004; accepted 18 March 2006

Abstract

The E-W to WNW-ESE striking Kunlun Fault Zone, extending about 1600 km, is one of the large strike-slip faults in the northern Tibet, China. As a major strike-slip fault, it plays an important role on the extrusion of Tibet Plateau in accommodating northeastward shortening caused by the India-Asia convergence. However, the time of initiation left-lateral faulting of the Kunlun Fault Zone is still largely debated, ranging from the Middle to Late Triassic (240–200 Ma) to early Quaternary (2 Ma). We document displaced basement rocks and geomorphic features along the Kunlun Fault Zone, based on tectono-geomorphic interpretation of satellite remote sensing images and field geologic and geomorphic observations. Our results show that the largest cumulative offset of basement rocks is likely to be 100 ± 20 km. Meanwhile, a series of pull-apart basins (Kusai, Xiugou and Tuosu lake basins) and pressure ridges (East Deshuiwai and Maji Snow Mountains), each 45–70 km long and ~8–12 km wide, are developed along the Kunlun Fault Zone, which resulted from long-term tectono-geomorphic growth since the Late Miocene or Early Pliocene. Geologic evidence indicates that the Kunlun Fault Zone had a long-term slip rate of ca.10 mm/yr during the late Quaternary. This slip rate is similar to that shown by present-day GPS measurements. Thus, we estimate that the Kunlun Fault Zone probably began left-lateral faulting at 10 ± 2 Ma based on a total displacement of 100 ± 20 km, and assuming a constant long-term slip rate of ca.10 mm/yr for several millions of years. And this timing constraint on initiation of left-lateral faulting of the Kunlun Fault Zone is consistent with widespread tectonic deformation which occurred in the Tibetan Plateau.

Keywords: Left-lateral faulting; Displaced basement rocks; Pull-apart basin; Pressure ridge; Kunlun Fault Zone; Northern Tibet

1. Introduction

The Cenozoic deformation of the Tibetan Plateau is dominated by the effects of the India-Asia collision, which resulted in the construction of its imposing topography (Molnar and Tapponnier, 1975; Yin and Harrison, 2000) (Figs. 1a,b). In northern Tibet, the Kunlun and the Altyn Tagh faults are two major strike-slip faults that help accommodate the ongoing collision between the Indian and Asian tectonic plates (Fig. 1a; Molnar and Tapponnier, 1975, 1978; Avouac and Tapponnier, 1993). A number of studies reveal that the Altyn Tagh fault underwent a total displacement of 470 ± 70 km and began left-lateral fault movement at 49 Ma (Yin et al., 2002), and it, thus, has a long-term slip rate of 9–10 mm/yr (Wang, 1997; Yin et al., 2002). This long-term slip rate estimated from geologic data is similar to the rate shown by GPS measurements (Bendick et al., 2000). However, an important tectonic element in the India-Asia collision system, the timing of left-lateral faulting for the Kunlun Fault Zone,

* Corresponding author. Tel.: +86 10 6200 7972; fax: +86 10 6201 0846.
E-mail address: fubihong@mail.iggcas.ac.cn (B. Fu).

1367-9120/$ - see front matter
doi:10.1016/j.jseaes.2006.03.004

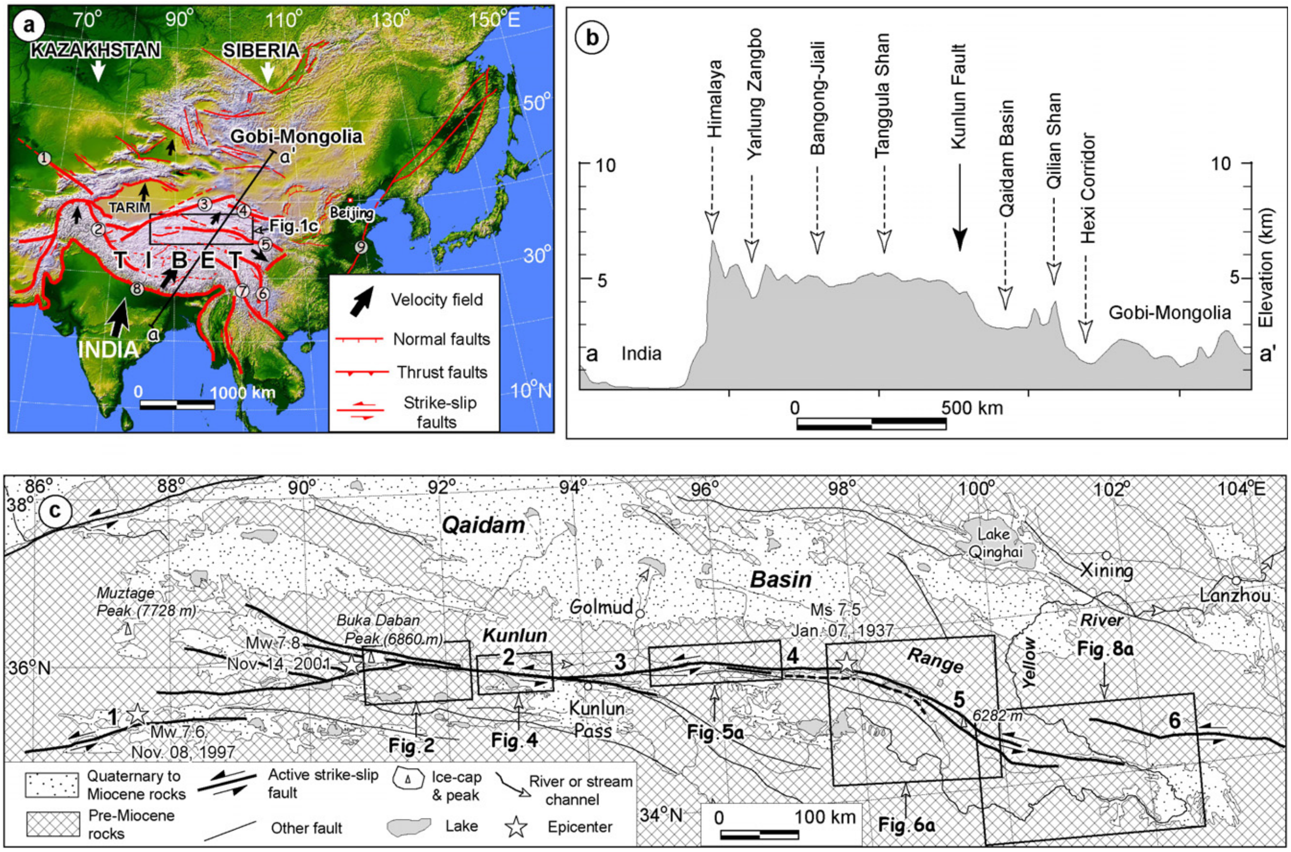

Fig. 1. (a) Cenozoic tectonic and topographical map of the India-Asia collision zone (Main tectonic elements are modified from Tapponnier et al., 2001). Topographic map generated from the USGS Shuttle Radar Topography Mission (SRTM) digital elevation models (DEMs). (b) Topographic profile across the India, Tibetan Plateau and Gobi-Mongolia region. Location of profile see a–a′ in (a). (c) Simplified tectonic map of the Kunlun Fault System between 86° and 104°E (modified from CIGMR, 2004). 1, Manyi segment; 2, Kusai Lake-Kunlun Pass segment; 3, Xitatan-Dongtatan segment; 4, Tuosu Lake segment; 5, Maqu segment; 6, Min Shan segment.

is still largely debated. According to evidence from mylonite and granite developed along the fault zone, Xu et al. (1997) infer that the Kunlun Fault Zone commenced sinistral shear movement in the Middle to Late Triassic (240–200 Ma). Other researchers (e.g. Meyer et al., 1998; Jolivet et al., 2003) suggest that the initiation of the Kunlun strike fault was early Neogene in age, based on the analysis of geological features in the Jingyu Basin and the intrusion of Tertiary to Quaternary shoshonites in the western part of Kunlun Fault System. In contrast to above scenarios, other workers have suggested that the Kunlun Fault System began its left-lateral motion in the Pliocene or early Pleistocene (Kidd and Molnar, 1988; Wu et al., 2001), on the basis of the geological and geomorphological features of the Kunlun Pass basin. It is necessary to find new evidence to constrain more reliable age of initiation of the left-lateral faulting along the Kunlun Fault Zone, and this also has important implications for understanding the tectono-geomorphological development and tectonic evolution of the northern part of the Tibetan Plateau.

To constrain the timing of left-lateral faulting and the total amount of left-lateral displacement of the Kunlun Fault Zone, we have studied the geological and geomorphological features along the Kunlun Fault Zone from the tectono-geomorphic interpretation of satellite remote sensing images and Shuttle Radar Topography Mission (SRTM) digital elevation model (DEM) data, as well as from field investigations.

2. Geological setting

The Kunlun Fault Zone, a major tectonic boundary in northern Tibet, is a Paleozoic suture zone (Tapponnier et al., 2001; Bian et al., 2004). This fault zone has been regarded as a lithospheric-scale strike-slip fault (Meyer et al., 1998; Kind et al., 2002). Northeastward convergence between Tibetan Plateau and Gobi-Mongolia is largely partitioned by the left-lateral slip of the Kunlun and Altyn Tagh fault zones (Avouac and Tapponnier, 1993; Meyer et al., 1998).

The main trace of the Kunlun Fault Zone, extending about 1600 km, is approximately parallel to the Kunlun Range (Fig. 1c). It may be roughly divided into six segments, each 150–350 km long, on the basis of the geometry of the fault trace and the structural assemblage (QHSB, 1999; Fu et al., 2005a) (Fig. 1c). Analysis of satellite images, cosmogenic surface dating, radiocarbon dating and trench surveys along the Kunlun Fault Zone suggest an average slip rate of 10–20 mm/yr during the Quaternary

(Kidd and Molnar, 1988; Zhao, 1996); or 11.5 ± 2 mm/yr during the past 40 kyr (Van der Woerd et al., 1998, 2002). Fu et al. (2005b) also determined a slip rate of 10 ± 1.0 mm/yr based on ^{14}C dating of offset fluvial fans during late Quaternary along the Kusai Lake-Kunlun Pass segment. Over the short-term, GPS data give a similar slip rate about 10 mm/yr (Wang et al., 2001; Zhang et al., 2004). Thus, both the geological and GPS data suggest that the Kunlun Fault has a uniform slip rate of ca.10 mm/yr.

The Kunlun Fault Zone is an active left-lateral strike-slip fault with dense seismic activity. Five large earthquakes ($M > 7.0$) have occurred along this fault zone during the past 100 years. The most recent earthquake occurred on November 14, 2001 (Lin et al., 2002; Fu et al., 2005a). A ~430 km long surface rupture zone was produced along the Kusai Lake-Kunlun Pass segment during the M_w 7.8 Kunlun earthquake with a maximum left-lateral displacement of ~8–10 m (Fu and Lin, 2003; Fu et al., 2005a). The 1997 M_w 7.6 Manyi earthquake broke the westernmost 170-km long Manyi segment between 86°30′E and 88°30′E (Fig. 1c), with a maximum left-lateral displacement of ~7 m (Peltzer et al., 1999). The 1973 M_s 7.4 Manyi earthquake occurred along the western part of the Manyi Fault. The length of surface rupture is unclear, although aftershocks extended for about 200 km along the fault (Velasco et al., 2000). The 1937 M_s 7.5 Tuosu Lake (or Huashixia) earthquake produced a rupture zone about 180 km long between 97°30′ E and 99°30′ E (Liu et al., 1996) (Fig. 1c) on the Tuosu Lake segment, with a maximum horizontal offset of ~6–7 m (Jia et al., 1988; QHSB, 1999). The 1963 M_s 7.0 Alake Lake earthquake ruptured the western part of the Tuosu Lake Fault (QHSB, 1999). There are no older historical records of earthquakes along the Xidatan-Dongdatan and Maqu segments although there are offset geomorphological features formed by past seismic events (Kidd and Molnar, 1988; Van der Woerd et al., 1998, 2002). Trenching survey studies and offset geomorphological features suggest that the recurrence interval of great earthquakes ($M \geqslant 7.5$) are ~850 and ~420 yrs with a characteristic slip of 10 ± 2 m and 4.4 ± 0.4 m for each event on the Xidatan-Dongdatan and Maqu segments, respectively (Zhao, 1996; Van der Woerd et al., 1998, 2002).

3. Displacement of basement rocks and long-term geomorphological features

Tectono-geomorphological interpretations of satellite remote sensing and SRTM relief-shaded images, as well as field observations, have been used to identify geological and geomorphological features along the Kunlun Fault Zone.

3.1. Buka Daban-Hongshui River area

To the east of Buka Daban Peak, the highest peak along the Kunlun Fault Zone, the fault trace exhibits as a sharp lineament on the satellite image (Fig. 2a). Geomorphologically, it forms a long and narrow valley between the Buka Daban Peak and Hongshui River (Fig. 2a). Oligocene sedimentary rocks are distributed on both sides of the fault zone (Fig. 2b; Zhang and Zheng, 1994). As shown on Fig. 2b, there are two possible interpretations of the displacement of the Oligocene sedimentary rocks: one of them proposes that A–A′ and B–B′ can be matched; the lateral offsets are 50 ± 5 km to 55 ± 5 km, respectively. A second possible explanation is that A–B′ are piercing points and the Oligocene sequence has undergone a lateral offset of 85 ± 10 km. The three-dimensional (3D) perspective ASTER image shows that Oligocene sedimentary rocks, yellow to yellowish green in the satellite images, have been cut by the Kunlun Fault (Fig. 3). As we have observed in the field, the Oligocene sequences in this region consist of red sandstones and argillites containing gypsum (Zhang and Zheng, 1994).

3.2. Kusai Lake area

In the Kusai Lake region, we can also observe from satellite imagery that the Triassic sequence is distributed on both sides of the Kunlun Fault (Fig. 4a). The displacement of Mid-Triassic rocks is at least 45 ± 2.5 km (Fig. 4b). It is possible that the displacement of Triassic sequence across the fault zone exceeds 45 ± 2.5 km because the Triassic sequences on the southern side of the fault have not been preserved. Kidd and Molnar (1988) inferred that lateral offset of the Triassic unit is about 70 km in the Kusai Lake region. In this region, the Mid-Triassic Gangde Formation is characterized by grey to greyish green sandstone with sandy limestone, phyllite or slate. The Gangde Formation contains conodont fossils, such as *Neogondollea mombergensis* (Tage), *Neogondollea transita* (Kozur et Moster) and *Galdigondolella tethydis* (Huckriede), and, thus, was assigned a mid-Triassic age (Zhang and Zheng, 1994). Kusai Lake, 45-km long and 8-km wide, lies within an asymmetric rhomb-shaped basin (Fig. 4). Geometry and tectono-geomorphological features suggest that formation and evolution of the Kusai Lake was controlled by strike-slip faulting along the Kunlun Fault Zone. At a different scale, rivers or their channels show systematically left-lateral offset across the fault zone (Fig. 4), caused by cumulative offsets since ~140 ka (Fu et al., 2005b).

3.3. Xiugou area

The relief-shaded image generated from the SRTM DEM data provides a useful tool for mapping topographic features along the Kunlun Fault Zone. In the Xiugou area, the large almond-shaped Xiugou Basin appears as a depression, 70-km long and 12-km wide (Fig. 5a). To east of this basin, there is an high almond-shaped topographic feature (East Deshuiwai Mountain) of a similar size to the Xiugou Basin (Fig. 5a). We interpret these features as a pull-apart basin and a pressure ridge, formed in releasing and restraining bends (Fig. 5a). Oligocene to Miocene sedimentary rocks are widely exposed in the Xiugou region (Fig. 5b; CIGMR, 2004). The distribution of the

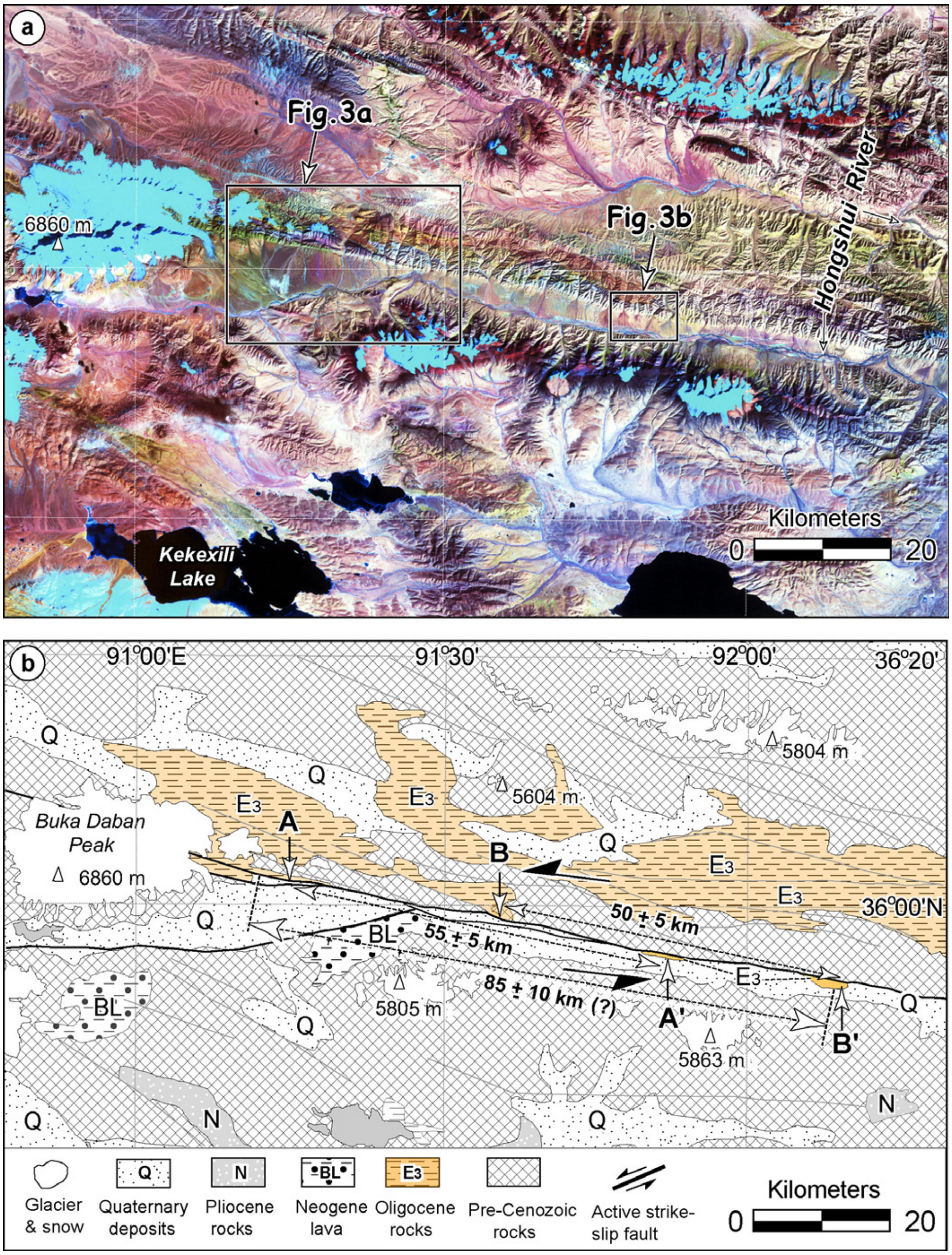

Fig. 2. (a) Landsat TM mosaic image of the east Buka Daban region, Kunlun Fault. (b) Geological interpretation showing the displacement of Tertiary sedimentary rocks along the fault. For location see Fig. 1c.

Oligo-Miocene deposits is not controlled by the faults bounding the pull-apart basin (Fig. 5b). The oldest sediments within the Xiugou pull-apart basin (Chengdu Institute of Geology and Mineral Reources – CIGMR, 2004), resting unconformably on Pre-Cenozoic rocks (QHSB, 1999), are Pliocene red beds.

3.4. Huashixia area

Further east in the Huashixia area, Tuosu Lake occupies a rhomb-shaped basin with a length of 60 km and a width of 10 km. To east of 99°E, the Kunlun Fault Zone changes strike to NW-SE, and the Maji Snow Mountain with a 6282 m peak appears as a high almond-shaped topographic feature (Fig. 6a). This topographic feature is 48-km long and 10-km wide, similar to the size of the Tuosu Lake Basin. We interpret these features as a pull-apart basin and a pressure ridge, bounded by left-lateral faults (Fig. 6b). The SRTM relief-shaded images clearly show that the Tuosu Lake Basin and Maji Snow Mountain are developed in a releasing step-over and a restraining bend, respectively (Fig. 7).

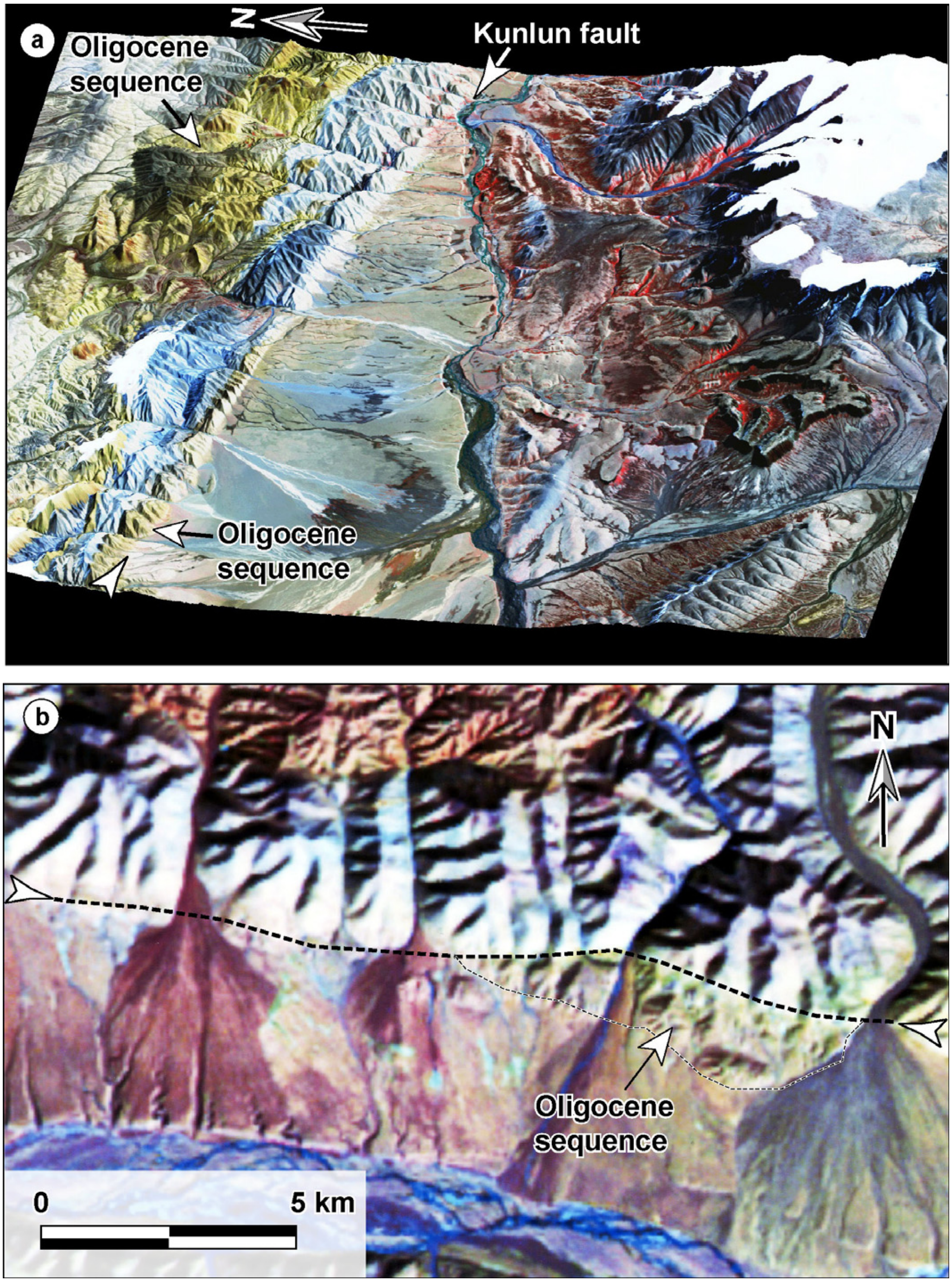

Fig. 3. (a) ASTER 3D perspective image showing Tertiary rocks to the southeast of Buka Daban Peak. (b) Landsat TM image showing Tertiary rocks on the south side of Kunlun Fault Zone. For locations see Fig. 2a.

3.5. Maqin-Maqu area

Even further eastward in the Maqin-Maqu area, the Maqu segment of Kunlun Fault continues striking NW-SE (Fig. 1c). The SRTM relief-shaded image shows that the Maqu segment has two main splays (Fig. 8a). River channels show left-lateral offset across the fault zone, and the Yellow River shows a ~90 km sinistral displacement along the northern strand of the fault (Fig. 8a). Van der Woerd et al. (2002) suggest that the 85–90 km displacement of Yellow River might represent total lateral offset of the Kunlun Fault Zone. Cretaceous sedimentary rocks are distributed on both sides of the Kunlun Fault (Fig. 8b). The Cretaceous sequences consist of grey, greyish green to greyish brown conglomerate and quartzose sandstone, containing the fossil lamellibranch *Musculus* sp. (Qinghai Bureau of Geology and Mineral Resources – QHBGMR, 1986b). Based on the geological and geometrical features of the Cretaceous rocks around the faults, we interpret that they were deposited within a

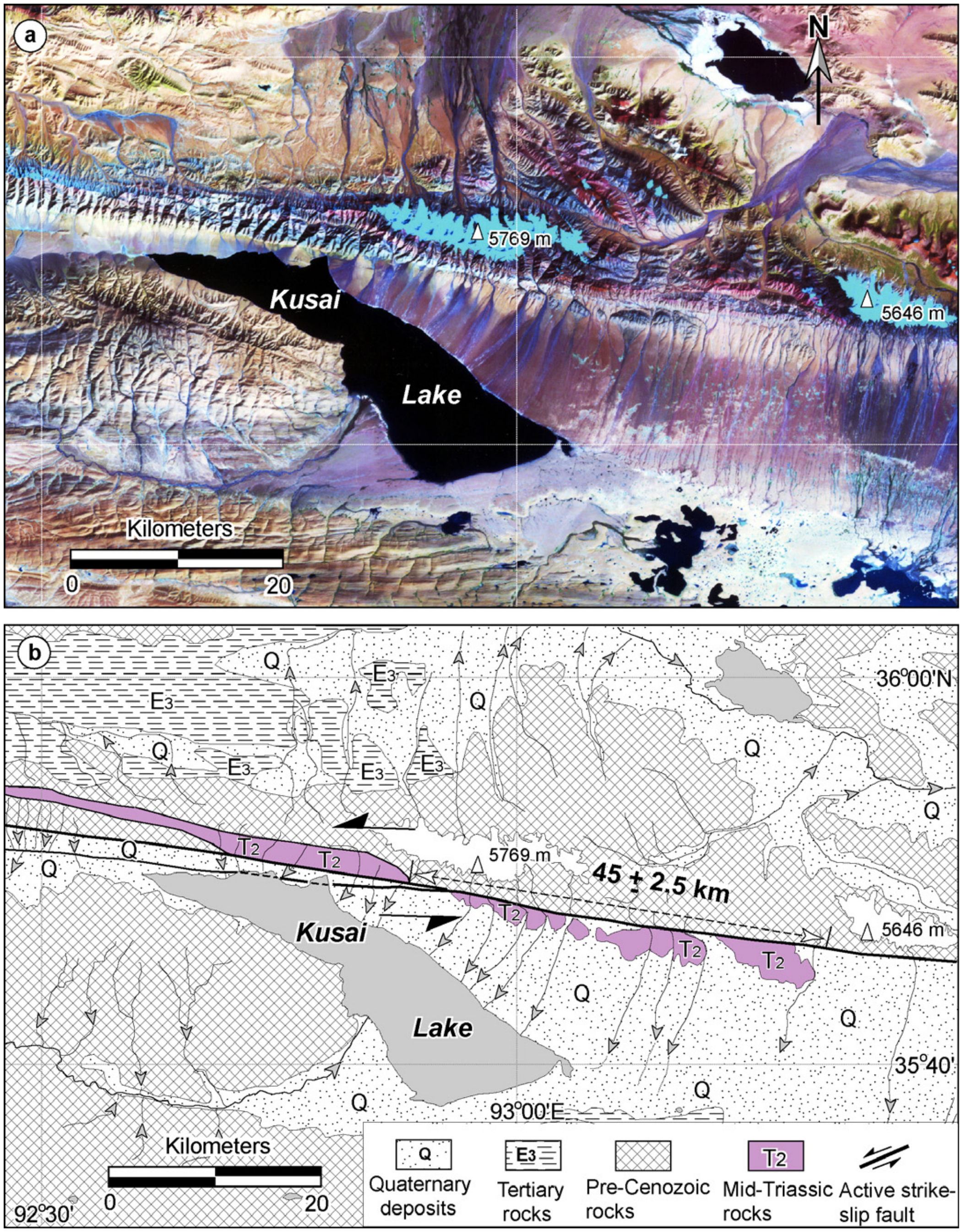

Fig. 4. (a) Landsat TM mosaic image of the Kusai Lake region. (b) Geological interpretation showing the displacement of Triassic rocks along the fault zone. For location see Fig. 1c.

continuous intramontane sedimentary basin, prior to the initiation of left-lateral faulting on the Kunlun Fault. The total displacement along the Kunlun Fault was determined by matching Cretaceous rocks across the faults (Fig. 8c). After the removal of ~120 km displacement along the fault zone, as shown in Fig. 8c, the Cretaceous rocks can be well matched. The total displacement of ~120 km may partition into offsets of 67.5 and 52.5 km along the northern and southeastern strands of the fault, respectively (Fig. 8c).

4. Discussion

4.1. Total displacement and timing of left-lateral fault movement

As described above, the Cretaceous rocks in the Maqin-Maqu area probably record a 120 km displacement along the Kunlun Fault Zone (Fig. 8c). Similarly, the Oligocene sedimentary rocks in the Buka Daban-Hongshui River area may have undergone left-lateral displacement of

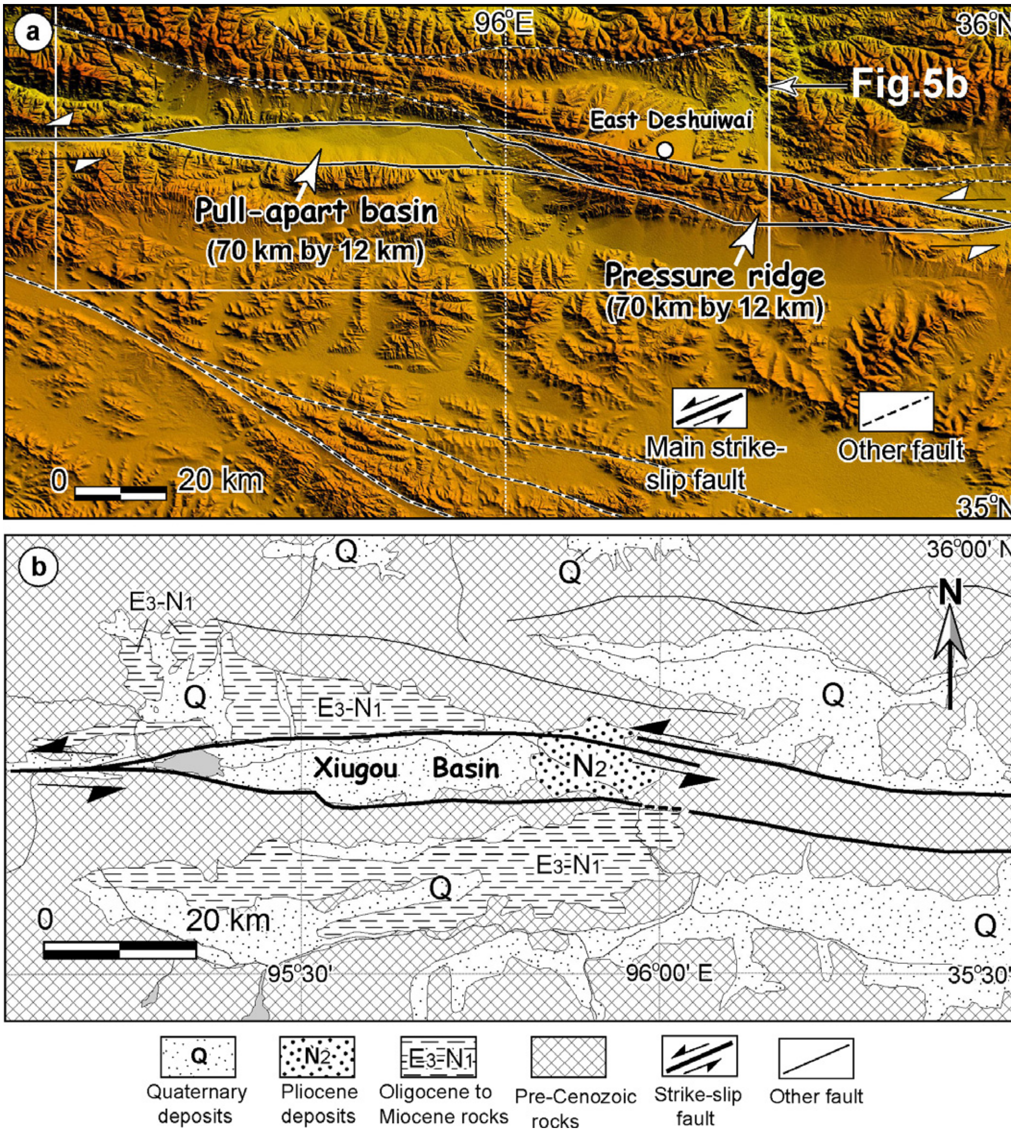

Fig. 5. (a) SRTM relief-shaded image showing topographic features of the Xiugou area. (b) Geological interpretation showing geological and geomorphological features of the pull-apart basin along the fault zone. Geological interpretation from Landsat ETM image and published geological data (after CIGMR, 2004; QHBGMR, 1986a). For location see Fig. 5a.

85 ± 10 km (Fig. 2b). Xu et al. (1997) estimate that in the Xidatan-Dongdatan segment the total displacement is at least 80 km, based on a calculation of ductile shear deformation. Thus, the displacement of 100 ± 20 km recorded by these Pre-Quaternary basement rocks most likely represents the maximum offset or the total displacement along the Kunlun Fault Zone.

Previous workers have inferred that in the eastern part of Kunlun Fault Zone the greatest offset of the Yellow River across the fault zone is about 85 km (Van der Woerd et al., 2002). However, this interpretation has much uncertainty because in this segment the Kunlun Fault Zone splits into two main strands (Fig. 8a). In the Kunlun Pass area, previous studies indicate that Late Pliocene or early Pleistocene moraine deposits containing pyroxenite boulders is separated by 30 km from the nearest rock outcrop (Kidd and Molnar, 1988). The offset of 30 km may present the total offset since the Late Pliocene or early Pleistocene (Kidd and Molnar, 1988). Therefore, we believe that total offset is most likely 100 ± 20 km since the initiation of left-lateral motion along the Kunlun Fault Zone.

Based on geological evidence, the long-term slip rate of the Kunlun Fault Zone is ca.10 mm/yr (Zhao, 1996; Van der Woerd et al., 1998, 2002; Fu et al., 2005b). GPS data also show a similar slip rate of about 10 mm/yr along the fault zone at the present-day (Wang et al., 2001; Zhang et al., 2004). Assuming that 10 mm/yr lateral slip rate continued for several millions of years, the left-lateral motion of the Kunlun Fault Zone must have commenced at 10 ± 2 Ma (Late Miocene). Previous workers (e.g. Jolivet et al., 2003) inferred that the Kunlun Fault Zone may have begun left-lateral fault movement in the early Neogene (ca.15 Ma) because the Jingyu basin, a pull-apart basin in the western Kunlun ranges, started to form around

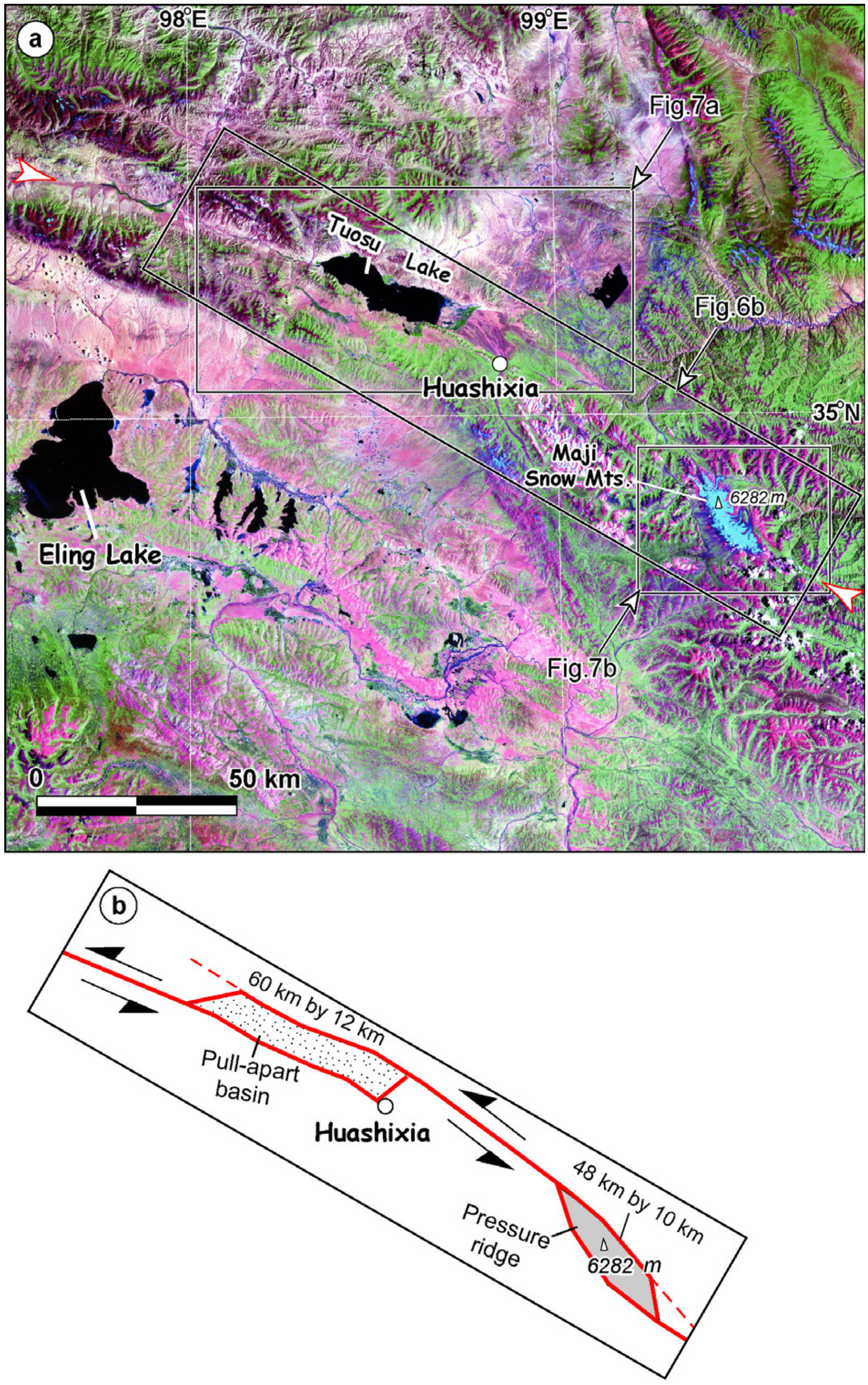

Fig. 6. (a) Landsat TM mosaic image of the Tuosu Lake segment, Kunlun Fault. For location see Fig. 1c. (b) Geological interpretation showing the structural features of pull-apart basin and pressure-ridge along the fault. For location see (a).

15 Ma; the left-lateral movement along the Kunlun Fault Zone may have been initiated in the same period. Moreover, shoshonitic lavas with an age range from 15 to 1.21 Ma distributed in this region (Jolivet et al., 2003), indicate an extensional tectonic environment. However, these Miocene to Pleistocene volcanic eruptions suggest only multiple tectonic activity in northern Tibet, and may not simply represent the initiation of left-lateral faulting along the Kunlun Fault Zone (Yang et al., 2002).

A number of studies reveal the tectonic changes which occurred in the Tibet Plateau-Himalayan orogen during the Late Miocene and Early Pliocene. In the Himalayas the drainage system changed between 7.5 and 6.5 Ma, associated with tectonic movements (Amano and Taira, 1992).

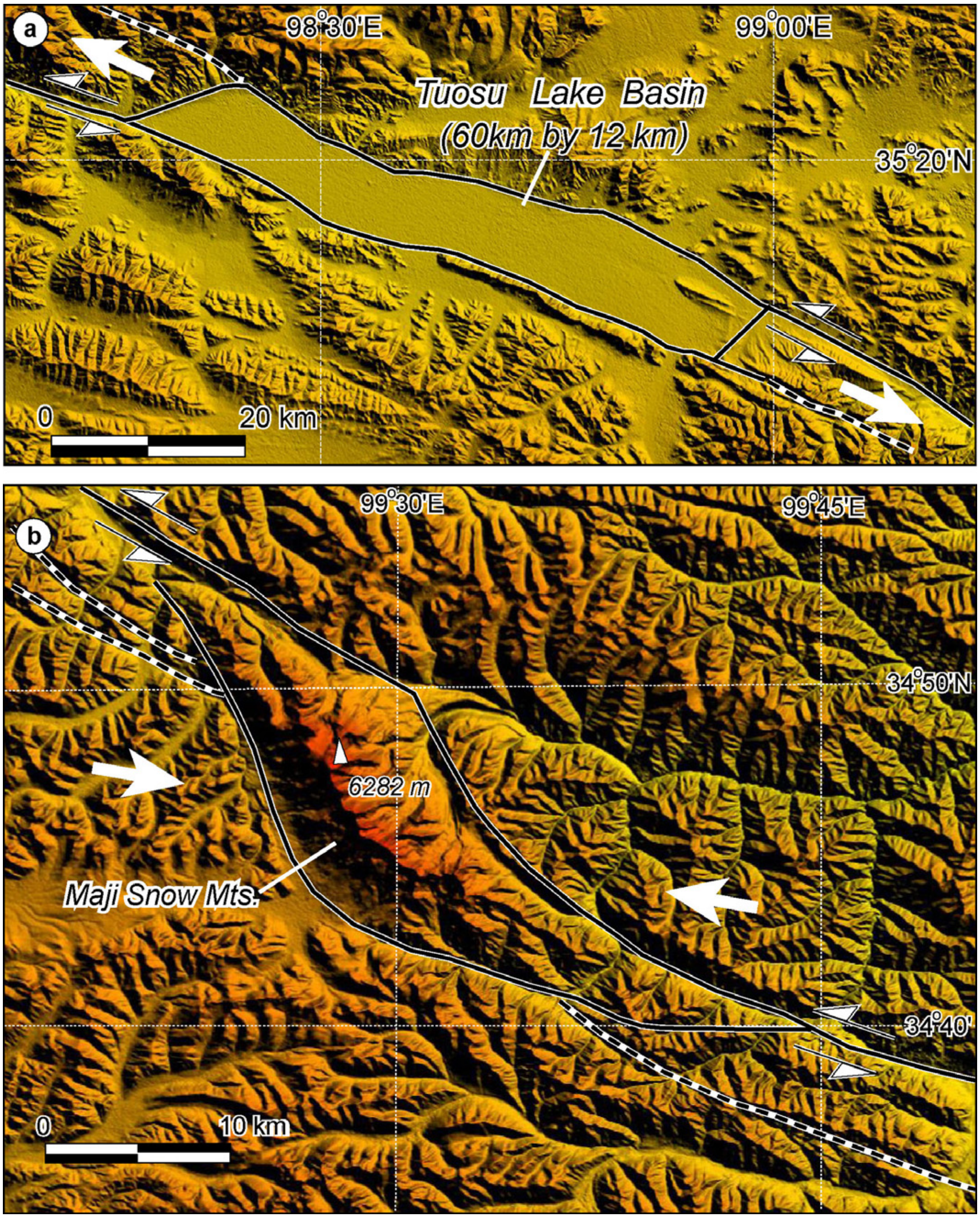

Fig. 7. SRTM DEM shaded-relief image showing the geomorphological features of the pull-apart basin and pressure ridge in the Tuosu lake segment. (a) The Tuosu Lake Basin appearing as a low rhomb-shaped topographic feature bounded by strike-slip faults. (b) The Maji Snow Mountain showing a high almond-shaped topographic feature. For locations see Fig. 6a.

Mercier et al. (1987) showed that the tectonic regime changed from a compression to extension in Tibet during the Late Miocene to Early Pliocene (10–5 Ma). In central to northern Tibet, extensional rifting may have developed later than 10 Ma (Yin et al., 1999). In the northeastern part of Tibet, the Altyn Tagh Fault transformed to the second stage of fault movement ca.13–16 Ma (Yue and Liou, 1999; Sun et al., 2005). The right-lateral Wenquan Fault is regarded as having commenced strike-slip motion in the Late Miocene to Pliocene (Wang and Burchfiel, 2004), and the Haiyuan Fault Zone has also been inferred to have begun left-lateral fault movement in the Late Miocene (Ding et al., 2004). In southeastern Tibet, many researchers infer that rapid uplift and river incision occurred in the Late Miocene or Early Pliocene (7–13 Ma), as implied by the rapid cooling history (e.g. Kirby et al., 2002; Clark et al., 2004). All of these facts indicate that tectonic changes in the Late Miocene or Early Pliocene had widespread effects on tectonic deformation in the India-Asia collision zone. Thus, timing of the initiation of left-lateral motion along the Kunlun Fault Zone is consistent with tectonic changes which occurred during the Late Miocene to Early Pliocene in the India-Asia collision zone.

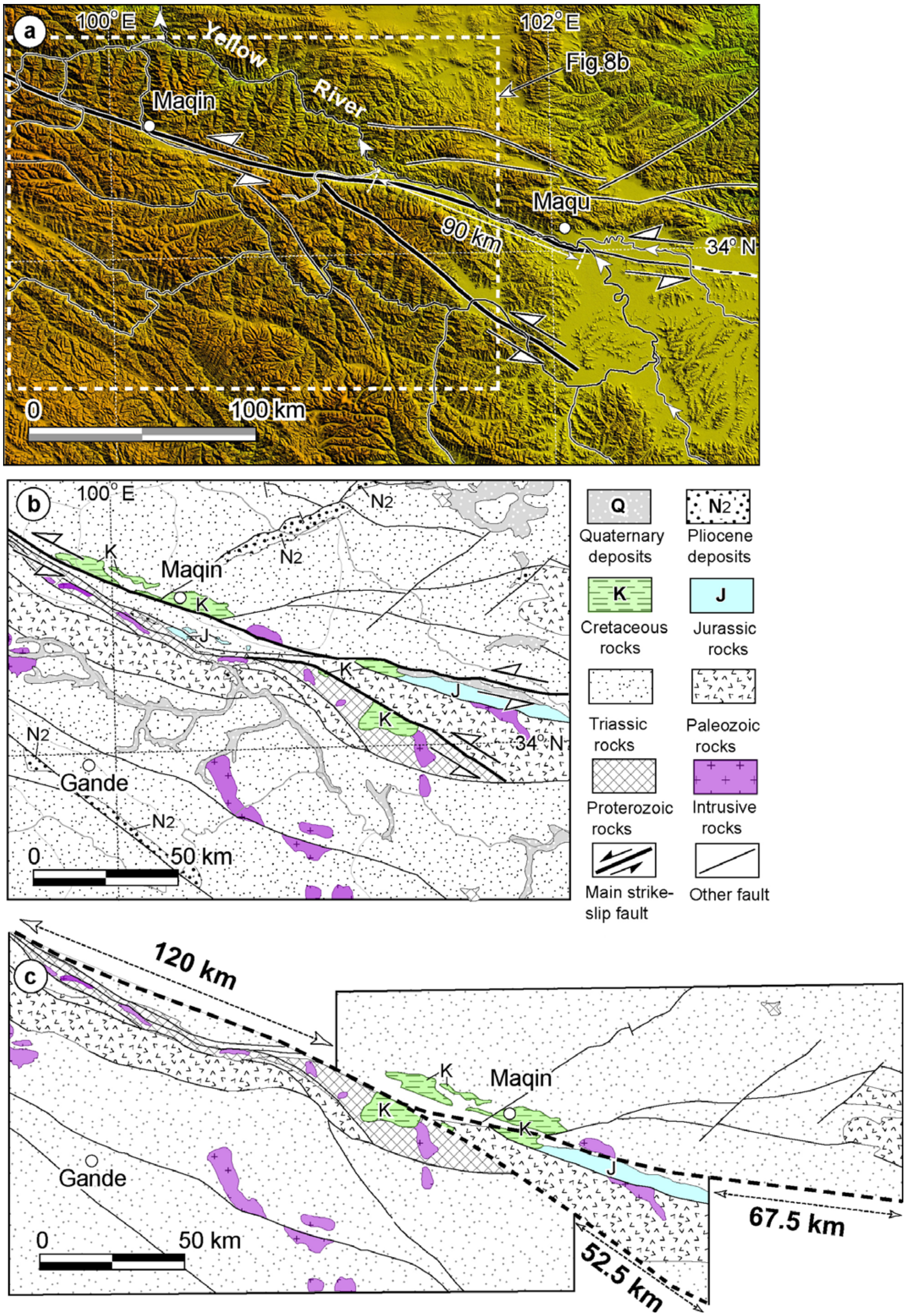

Fig. 8. (a) SRTM DEM shaded-relief image showing geomorphological features of the Maqin segment, Kunlun Fault. Note the Yellow River has a left-lateral offset of ~90 km. For location see Fig. 1c. (b) Geologic map showing distribution of Cretaceous sedimentary rocks on both sides of strike-slip faults (after CIGMR, 2004; QHBGMR, 1986b). For location see (a). (c) Reconstructed geological features after restoring a horizontal offset of 120 km along the fault zone.

4.2. Tectono-geomorphic growth of the Kunlun Fault Zone

Previous studies have recognized a variety of fault-bounded structures, including systematically deflected streams, shutter ridges, displaced fluvial fans, pressure ridges and sag-ponds (or grabens) along the Kunlun Fault Zone during the Quaternary (Kidd and Molnar, 1988; Zhao, 1996; Van der Woerd et al., 1998, 2002; Fu et al., 2005b). As described in this study, we have mapped the large-scale displacement of basement rocks, pull-apart basins and pressure ridges developed along the Kunlun Fault Zone (Figs. 2, 4–7, and 8).

A number of studies suggest that the growth of fault-bounded geologic structures is caused mainly by repeated large seismic events (e.g. King et al., 1988; Bilham and King, 1989), and this assumption has been confirmed by field examples (Stein et al., 1988; Bilham and King, 1989). Tectono-geomorphological features along a strike-slip fault typically grow with time (e.g. Wallace, 1968; Sylvester, 1988). However, the preservation of these long-term geologic and geomorphic features is complex, because they are strongly affected by the local conditions such as lithology, topography and climate, as well as by tectonic forcing (Bull and Knuepfer, 1987; Burbank and Anderson, 2001). Long-term tectono-geomorphological features along a strike-slip fault trace can be preserved if a balance between erosion and sedimentation processes and strike-slip motions along fault zone is achieved (Lacassin et al., 1998; Burbank and Anderson, 2001). Large-scale displaced outcrops and the deflection of rivers over several tens or hundreds of kilometers are found to have developed along large strike-slip faults in the Tibetan Plateau, such as the Altyn Tagh Fault (Wang, 1997; Meng et al., 2001; Yin et al., 2002), the Red River Fault (Replumaz et al., 2001), Xianshui River-Xiaojiang Fault (Wang et al., 1998), and the Karakorum Fault (Murphy et al., 2000). In general, displaced basement rocks and offset streams or rivers across strike-slip faults are good markers for recording the true tectonic offset along the fault zone (Gaudemer et al., 1989; Wang, 1997; Yin et al., 2002).

Similarly, our results demonstrate that a series of large-scale pull-apart basins and pressure ridges, each 45–70 km long and 8–12 km wide, are well developed along the Kunlun Fault Zone (Figs. 4–7). The geometry and evolution of pull-apart basins and pressure ridges along the Kunlun Fault Zone are obviously controlled by releasing and restraining step-overs or bends (Figs. 5–7). Geometry, geomorphological features and the progressive evolution of pull-apart basins and pressure ridges have been noted in a number of previous studies (Aydin and Nur, 1982; Dooley and McClay, 1997; McClay and Bonora, 2001). One simple model shows how the length and width of the pull-apart basin along the strike-slip fault increases with increasing horizontal displacement (Fig. 9). Similarly, pressure ridges or push-ups along strike-slip faults must also tend to grow with time (e.g. Aydin and Nur, 1982; Cowgill et al., 2004a,b). Geological data show that the oldest sedimentary sequence within these pull-apart basins is of Pliocene age (Fig. 5b; CIGMR, 2004), which implies that these large-scale pull-apart basins formed in the Late Miocene or Early Pliocene. Large-scale pressure ridges, each 50–70 km long and 8–12 km wide, also started to form at the same time.

5. Conclusions

Geological and geomorphological features provide good markers to constrain the major offset along the Kunlun Fault Zone. Displaced basement rocks show a total offset of 100 ± 20 km. Similarly, a series of pull-apart basins and pressure ridges 45–70 km long and ~8–12 km wide are developed along the Kunlun Fault Zone, which resulted from long-term tectono-geomorphological growth. Geological evidence indicates that the Kunlun Fault has had a uniform slip rate of 10–12 mm/yr during the Late Quaternary. This slip rate is similar to that reported from present-day GPS measurements. Thus, we can infer that the Kunlun Fault Zone probably began left-lateral fault movement in the Late Miocene (10 ± 2 Ma) based on a total displacement of 100 ± 20 km and a long-term slip rate of ca.10 mm/yr. This time constraint on initiation of left-lateral strike-slip faulting along the Kunlun Fault Zone is consistent with the widespread tectonic deformation which has occurred in the Himalayas and on the Tibetan Plateau.

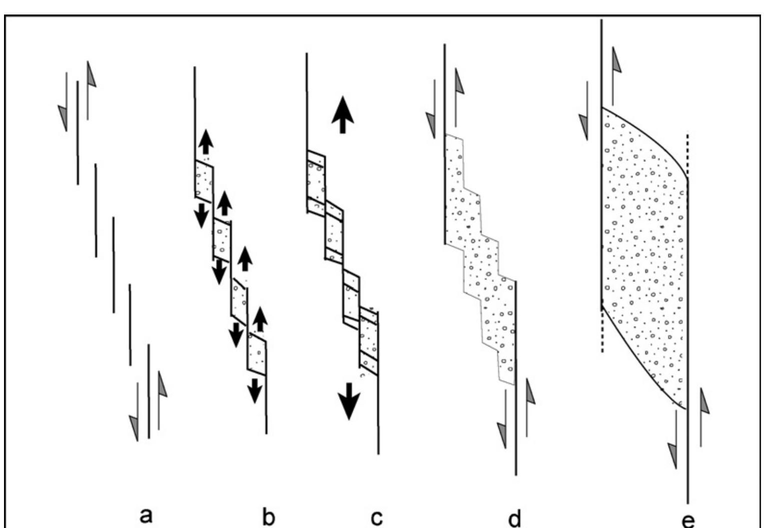

Fig. 9. Model illustrating coalescence of rhomb-shaped grabens associated with en echelon strike-slip faults. The end product is a composite pull-apart basin (modified after Aydin and Nur, 1982). Note that increased displacement causes the length and width of graben basin to increase with time.

This study case, thus, provides a good example for understanding the long-term tectono-geomorphological evolution of a major intracontinental strike-slip fault.

Acknowledgements

We thank R.S. Yeats and E. Kirby for critical and helpful reviews. Discussion with A. Yin and E. Wang improved the manuscript. ASTER remote sensing data were provided by the Earth Remote Sensing Data Analysis Center (ERSDAC), Japan. ER-Mapper software was used for satellite image processing. This research was funded by the research project from President Foundation of Chinese Academy of Sciences.

References

Amano, K., Taira, A., 1992. Two-phase uplift of Higher Himalayas since 17 Ma. Geology 20, 391–394.

Avouac, J.P., Tapponnier, P., 1993. Kinematic model of active deformation in central Asia. Geophysical Research Letters 20, 895–898.

Aydin, A., Nur, A., 1982. Evolution of pull-apart basins and their scale independence. Tectonics 1, 91–105.

Bendick, R., Bilham, R., Freymuller, J., Larson, K., Yin, G., 2000. Geodetic evidence for a low slip rate in the Altyn Tagh fault system. Nature 404, 69–72.

Bian, Q., Li, D., Pospelov, I., Yin, L., Li, H., Zhao, D., Chang, C., Luo, X., Gao, S., Astrakhantsev, O., Chamov, N., 2004. Age, geochemistry and tectonic setting of Buqingshan ophiolites, North Qinghai-Tibet Plateau, China. Journal of Asian Earth Sciences 23, 577–596.

Bilham, R., King, G.C.P., 1989. The morphology of strike-slip faults: examples from the San Andreas Fault, California. Journal of Geophysical Research 94, 10204–10216.

Bull, W.B., Knuepfer, P.L.K., 1987. Adjustments of the Charwell River, New Zealand to uplift and climatic changes. Geomorphology 1, 15–32.

Burbank, D.W., Anderson, R.S., 2001. Tectonic geomorphology. Blackwell Science, Massachusetts, p. 274.

Chengdu Institute of Geology and Mineral Resources of China Geological Survey (CIGMR), 2004. Geological map of Qinghai-Tibet Plateau and adjacent region (scale: 1:1,500,000). Chengdu Cartographic Publishing House.

Clark, M.K., Schoenbohm, L.M., Royden, L.H., Whipple, K.X., Burchfiel, B.C., Zhang, X., Tang, W., Wang, E., Chen, L., 2004. Surface uplift, tectonics, and erosion of eastern Tibet from large-scale drainage patterns. Tectonics, 23. doi:10.1029/2002TC001402.

Cowgill, E., Arrowsmith, J.R., Yin, A., Wang, X., Zhang, S., 2004a. The Akato Tagh bend along the Altyn Tagh fault, northwest Tibet 1: Smoothing by vertical-axis rotation and the effect of topographic stresses on bend-flanking faults. Geological Society of America Bulletin 116, 1423–1442.

Cowgill, E., Arrowsmith, J.R., Yin, A., Wang, X., Chen, Z., 2004b. The Akato Tagh bend along the Altyn Tagh fault, northwest Tibet 2: Active deformation and the importance of transpression and strain hardening within the Altyn Tagh system. Geological Society of America Bulletin 116, 1443–1464.

Ding, G., Chen, J., Tian, Q., Shen, X., Xing, C., Wei, K., 2004. Active faults and magnitudes of left-lateral displacement along the northern margin of the Tibetan Plateau. Tectonophysics 380, 243–260.

Dooley, T., McClay, K., 1997. Analog modeling of pull-apart basins. American Association of Petroleum Geologists Bulletin 81, 1804–1826.

Fu, B., Lin, A., 2003. Spatial distribution of the surface rupture zone associated with the 2001 M_s8.1 Central Kunlun earthquake, northern Tibet, revealed by satellite remote sensing data. International Journal of Remote Sensing 24, 2191–2198.

Fu, B., Awata, Y., Du, J., Ninomiya, Y., He, W., 2005a. Complex geometry and segmentation of the surface rupture associated with the 14 November 2001 great Kunlun earthquake, northern Tibet, China. Tectonophysics 407, 43–63.

Fu, B., Awata, Y., Du, J., He, W., 2005b. Late Quaternary systematic stream offsets caused by repeated large seismic events along the Kunlun Fault, northern Tibet. Geomorphology 71, 278–292.

Gaudemer, Y., Tapponnier, T., Turcotte, D., 1989. River offsets across active strike-slip faults. Annales Tectonicae 3, 55–76.

Jia, Y., Dai, H., Su, X., 1988. Tuosuo Lake earthquake fault in Qinghai Province. In: Xinjiang, S.B. (Ed.), Research on Earthquake Faults in China. Xinjiang People's Press, Urumqi, pp. 66–71 (in Chinese).

Jolivet, M., Brunel, M., Seward, D., Xu, Z., Yang, J., Malavieille, J., Roger, F., Lereloup, A., Arnaud, N., Wu, C., 2003. Neogene extension and volcanism in the Kunlun Fault Zone, northern Tibet: new constraints on the age of the Kunlun Fault. Tectonics, 22. doi:10.1029/2002TC001428.

Kidd, W.S.F., Molnar, P., 1988. Quaternary and active faulting observed on the 1985 Academia Sinica-Royal Society geotranverse of Tibet. Philosophical Transactions of The Royal Society of London (Series A) 327, 337–363.

Kind, R., Yuan, X., Saul, J., Nelson, D., Sobolev, S.V., Mechie, J., Zhao, W., Kosarev, G., Ni, J., Achauer, U., Jiang, M., 2002. Seismic images of crust and upper mantle beneath Tibet: Evidence for Eurasian plate subduction. Science 298, 1219–1221.

King, G.C.P., Stein, R.S., Rundle, J.B., 1988. The growth of geological structures by repeated earthquakes: 1. Conceptual framework. Journal of Geophysical Research 93, 13307–13318.

Kirby, E., Reiners, P.W., Krol, M.A., Whipple, K.X., Hodges, K.V., Farley, K.A., Tang, W., Chen, Z., 2002. Late Cenozoic evolution of eastern margin of the Tibetan Plateau: inferences from $^{40}Ar/^{39}Ar$ and (U/Th)/He thermochronology. Tectonics, 21. doi:10.1029/2000TC001246.

Lacassin, R., Replumaz, A., Leloup, P.H., 1998. Hairpin river loops and slip-sense inversion on southeast Asian strike-slip faults. Geology 26, 703–706.

Lin, A., Fu, B., Guo, J., Zeng, Q., Dang, G., He, W., Zhao, Y., 2002. Co-seismic strike-slip and rupture length produced by the 2001 M_s 8.1 Central Kunlun earthquake. Science 296, 2015–2017.

Liu, G.X., Xiao, Z.M., Xie, X.S., Tu, D.L., Zeng, Q.S., Wu, S.X., Zhang, R.B., Wang, H.Z., 1996. The surface rupture zone of the 1937 Huashixia earthquake ($M = 7.5$) in Qinghai. Research on Active Faults 5, 136–153.

McClay, K., Bonora, M., 2001. Analog models of restraining stopovers in strike-slip fault systems. American Association of Petroleum Geologists Bulletin 85, 233–260.

Meng, Q.R., Hu, J.M., Yang, F.Z., 2001. Timing and magnitude of displacement on the Altyn Tagh Fault: constraints from stratigraphic correlation of adjoining Tarim and Qaidam basins, NW China. Terra Nova 13, 86–91.

Mercier, J.L., Armijo, R., Tapponnier, P., Carey-Gailhardis, E., Han, T., 1987. Change from Late Tertiary compression to Quaternary extension in southern Tibet during the India-Asia collision. Tectonics 6, 275–304.

Meyer, B., Tapponnier, P., Bourjot, L., Metivier, F., Gaudemer, Y., Peltzer, G., Guo, S., Chen, Z., 1998. Crustal thickening in Gansu-Qinghai, lithospheric mantle subduction, and oblique, strike-slip controlled growth of the Tibetan plateau. Geophysical Journal International 135, 1–47.

Molnar, P., Tapponnier, P., 1975. Cenozoic tectonics of Asia: effects of a continental collision. Science 189, 419–426.

Molnar, P., Tapponnier, P., 1978. Active tectonics of Tibet. Journal of Geophysical Research 83, 5361–5375.

Murphy, M.A., Yin, A., Kapp, P., Harrison, T.M., Ding, L., Guo, J., 2000. Southward propagation of the Karakoram fault system, southwest Tibet: timing and magnitude of slip. Geology 28, 451–454.

Peltzer, G., Grampe, F., King, G., 1999. Evidence of nonlinear elasticity of the crust from the M_w 7.6 Manyi earthquake. Science 286, 272–276.

Qinghai Bureau of Geology and Mineral Resources (QHBGMR), 1986a. Geologic map of the Maduo County and Maji Snow Mountain Sheet (scale: 1:200,000). Geological Publishing House, Beijing.

Qinghai Bureau of Geology and Mineral Resources (QHBGMR), 1986b. Geologic map of the Youyun and Guolu Sheet (scale: 1:200,000). Geological Publishing House, Beijing.

Qinghai Seismological Bureau (QHSB), 1999. Eastern Kunlun active fault zone. Seismological Press, Beijing, 186pp.

Replumaz, A., Lacassin, R., Tapponnier, P., Leloup, P.H., 2001. Large river offsets and Plio-Quaternary dextral slip rate on the Red River fault (Yunnan, China). Journal of Geophysical Research 106, 819–836.

Stein, R.S., King, G.C.P., Rundle, J.B., 1988. The growth of geological structures by repeated earthquakes: 2. Field examples of continental dip-slip faults. Journal of Geophysical Research 93, 13319–13331.

Sun, J.M., Zhu, R.X., An, Z.S., 2005. Tectonic uplift in the northern Tibetan Plateau since 13.7 Ma ago inferred from molasse deposits along the Altyn Tagh Fault. Earth and Planetary Science Letters 235, 641–653.

Sylvester, A.G., 1988. Strike-slip faults. Geological Society of America Bulletin 100, 1666–1703.

Tapponnier, P., Xu, Z., Roger, F., Meyer, B., Arnaud, N., Wittlinger, Yang, J., 2001. Oblique stepwise rise and growth of the Tibet Plateau. Science 294, 1671–1677.

Van der Woerd, J., Ryerson, F.J., Tapponnier, P., Gaudemer, Y., Finkel, R.C., Meriaux, A.S., Caffee, M.W., Zhao, G., He, Q., 1998. Holocene left-lateral slip-rate determined by cosmogenic surface dating on the Xidatan segment of the Kunlun Fault (Qinghai, China). Geology 26, 695–698.

Van der Woerd, J., Tapponnier, P., Ryerson, F.J., Meriaux, A.S., Meyer, B., Gaudemer, Y., Finkel, R.C., Caffee, M.W., Zhao, G., Xu, Z., 2002. Uniform postglacial slip- rate along the central 600 km of the Kunlun Fault (Tibet), from ^{26}Al, ^{10}Be, and ^{14}C dating of riser offsets, and climatic origin of the regional morphology. Geophysical Journal International 148, 356–388.

Velasco, A.A., Ammon, C.J., Beck, S.L., 2000. Broadband source modeling of the November 8, 1997, Tibet ($Mw = 7.5$) earthquake and its tectonic implications. Journal of Geophysical Research 105, 28065–28080.

Wallace, R.E., 1968. Notes on stream channels offset by the San Andreas fault, southern Coast Ranges, California. In: Dickinson, W.R., Grantz, A. (Eds.), Conference on Geologic Problems of the San Andreas Fault System. Stanford University Publication in Geological Sciences, vol. 11, pp. 6–21.

Wang, E., 1997. Displacement and timing along the northern strand of the Altyn Tagh Fault Zone, Northern Tibet. Earth and Planetary Science Letters 150, 55–64.

Wang, E., Burchfiel, B.C., Royden, L.H., Chen, L., Chen, J., Li, W., Chen, Z., 1998. Late Cenozoic Xianshuihe-Xiaojiang, Red River, and Dali fault systems of southwestern Sichuan and central Yunnan, China. Geological Society of America Special Paper 327, 108 p.

Wang, E., Burchfiel, B.C., 2004. Late Cenozoic right-lateral movement along the Wenquan Fault and associated deformation: Implications for the kinematic history of the Qaidam Basin, northeastern Tibetan Plateau. International Geology Review 46, 861–879.

Wang, Q., Zhang, P., Freymuller, J.T., Bilham, R., Larson, K.M., Lai, X., You, X., Niu, Z., Wu, J., Li, Y., Liu, J., Yang, Z., Chen, Q., 2001. Present-day crustal deformation in China constrained by Global Positioning System measurements. Science 294, 574–577.

Wu, Y., Cui, Z., Liu, G., Ge, D., Yin, J., Xu, Q., Pang, Q., 2001. Quaternary geomorphological evolution of the Kunlun Pass area and uplift of the Qinghai-Xizang (Tibet) Plateau. Geomorphology 36, 203–216.

Xu, Z., Zhang, J., Xu, H., Wang, Z., Li, H., Yang, T., Qiu, X., Zeng, L., Shen, K., Chen, W., 1997. Ductile Shear Zones in the Main Continental Mountain Chains and their Dynamics. Geological Publishing House, Beijing, 294pp (in Chinese with English abstract).

Yang, J., Wu, C., Shi, R., Li, H., Xu, Z., Meng, F., 2002. Miocene and Pleistocene shoshonitic volcanic rocks in the Jingyuhu area, north of the Qinghai-Tibet Plateau. Acta Petrologica Sinica 18, 161–176.

Yin, A., Kapp, P.A., Murphy, M.A., Harrison, T.M., Grove, M., Ding, L., Deng, X., Wu, C., 1999. Significant late Neogene east-west extension in the northern Tibet. Geology 27, 787–790.

Yin, A., Harrison, T.M., 2000. Geologic evolution of the Himalayan-Tibetan orogen. Annual Review of Earth and Planetary Sciences 28, 211–280.

Yin, A., Rumelhart, P.E., Butler, R., Cowgill, E., Harrison, T.M., Foster, D.A., Ingersoll, R.V., Zhang, Q., Zhou, X., Wang, X., Hanson, A., Raza, A., 2002. Tectonic history of the Altyn Tagh Fault System in northern Tibet inferred from Cenozoic sedimentation. GSA Bulletin 114, 1257–1295.

Yue, Y., Liou, J.G., 1999. A two-stage evolution model for the Altyn Tagh Fault, China. Geology 27, 227–230.

Zhao, G., 1996. Quaternary faulting in the north Qinghai-Tibet Plateau. Earthquake Research in China 12, 107–119 (in Chinese with English abstract).

Zhang, P., Sheng, Z., Wang, M., Gan, W., Burgmann, R., Molnar, P., Wang, Q., Niu, Z., Sun, J., Wu, J., Sun, H., You, X., 2004. Continuous deformation of the Tibetan Plateau from global positioning system data. Geology 32, 809–812.

Zhang, Y., Zheng, J., 1994. Geological overview in Kokshili, Qinghai and adjacent areas (with geologic map 1:500,000). Seismological Press, Beijing, 177 pp.